Springer

Journal of Mechanical Science and Technology 23 (2009) 2502~2506

Journal of Mechanical Science and Technology

www.springerlink.com/content/1738-494x
DOI 10.1007/s12206-009-0709-5

Boundary treatment for the unsteady surface velocity in an immersed boundary method †

Seung Jeon and Haecheon Choi*

School of Mechanical and Aerospace Engineering, Seoul National University, Seoul 151-744, Korea

(Manuscript Received May 15, 2009; Revised May 26, 2009; Accepted May 26, 2009)

Abstract

In the present paper, we demonstrate that an unsteady velocity boundary condition on a solid surface induces artificial force oscillations on the solid body, and these oscillations can be effectively removed by imposing the Neumann boundary condition on the solid surface for the pseudo-pressure Poisson equation.

Keywords: Immersed boundary method; Artificial force oscillation; Poisson equation; Neumann boundary condition

1. Introduction

Since Peskin [1] first developed the immersed boundary (IB) method for flow over a complex geometry, various versions of immersed boundary methods have been developed aiming for better accuracy, simpler implementation, or less CPU time. A review on the immersed boundary method can be found in Mittal and Iaccarino [2]. In most studies on the immersed boundary method, however, the boundary condition on the solid boundary is steady, or focus is given to the flow field rather than to the force on the body even when the boundary condition on the solid surface is unsteady.

In the present paper, we show in the framework of the immersed boundary method (e.g., [3]) that artificial force oscillations on the body occur when an unsteady boundary condition is given at the solid boundary. These force oscillations are clearly non-physical and sometimes result in the blow-up of numerical solutions. We suggest a new boundary treatment for the pseudo-pressure Poisson equation, which is shown below, to remove effectively the artificial force oscillations on the body.

2. Violation of mass conservation

The governing equations for the unsteady incompressible flow are

$$\frac{\partial u_i}{\partial t}+\frac{\partial u_i u_j}{\partial x_j}=-\frac{\partial p}{\partial x_i}+\frac{1}{Re}\frac{\partial^2 u_i}{\partial x_j \partial x_j}+f_i, \tag{1}$$

$$\frac{\partial u_i}{\partial x_i}-q=0, \tag{2}$$

where t is time; x_i is the coordinate; u_i is the corresponding velocity component; p is the pressure; f_i and q are the momentum forcing and mass source/sink, respectively, proposed by [3]; and $Re= u_\infty d/\nu$ is the Reynolds number. Here, u_∞ is the free-stream velocity; d is the characteristic length; and ν is the kinematic viscosity. To solve Eqs. (1) and (2), a fractional step method is used together with a semi-implicit time advance scheme (a third-order Runge-Kutta method [RK3] for the convective term and a second-order Crank-Nicolson method for the diffusion term) as follows:

† This paper was recommended for publication in revised form by Associate Editor Dongshin Shin

*Corresponding author. Tel.: +82 2 880 8361, Fax.: +82 2 878 3662
E-mail address: choi@snu.ac.kr

$$\frac{\hat{u}_i^k - u_i^{k-1}}{\Delta t} = \alpha_k L\left(\hat{u}_i^k\right) + \alpha_k L\left(u_i^{k-1}\right) - 2\alpha_k \frac{\partial p^{k-1}}{\partial x_i} - \gamma_k N\left(u_i^{k-1}\right) - \rho_k N\left(u_i^{k-2}\right) + f_i^k, \tag{3}$$

$$\frac{\partial^2 \phi^k}{\partial x_i \partial x_i} = \frac{1}{2\alpha_k \Delta t}\left(\frac{\partial \hat{u}_i^k}{\partial x_i} - q^k\right), \tag{4}$$

$$u_i^k = \hat{u}_i^k - 2\alpha_k \Delta t \frac{\partial \phi^k}{\partial x_i}, \tag{5}$$

$$p^k = p^{k-1} + \phi^k - \frac{\alpha_k \Delta t}{Re}\frac{\partial^2 \phi^k}{\partial x_j \partial x_j}, \tag{6}$$

where $L(u_i)=(1/Re)\partial^2 u_i/\partial x_j \partial x_j$, $N(u_i)= \partial u_i u_j/\partial x_j$, $\hat{u}_i$ is the intermediate velocity; ϕ is the pseudo-pressure; Δt is the computational time step; k is the substep index; and α_k, γ_k, and ρ_k are the coefficients of RK3 ($\alpha_1 = 4/15,\ \gamma_1 = 8/15,\ \rho_1 = 0;\quad \alpha_2 = 1/15,\ \gamma_2 = 5/12,\ \rho_2 = -17/60;\ \alpha_3 = 1/6,\ \gamma_3 = 3/4,\ \rho_3 = -5/12$). The momentum forcing f_i is given on or near the immersed boundary to satisfy the no-slip velocity conditions, u_s and v_s, at the immersed boundary (Fig. 1).

The continuity equation should be satisfied for the cell containing the immersed boundary and for the fluid region in this numerical cell as well. From these constraints, one can obtain the amount of mass source/sink q as follows [3]:

$$q = \frac{1}{\Delta V}\sum_i \omega\left(\boldsymbol{u}^k - \boldsymbol{u}_s^k\right)\cdot \boldsymbol{n}\ \Delta S_i, \tag{7}$$

where ΔV is the cell volume; ΔS_i is the area of each cell face i; $\boldsymbol{u_s}$ is the surface velocity vector; and $\boldsymbol{n}$ is the unit normal vector outward of each cell face. Here, ω is defined as one for the cell faces

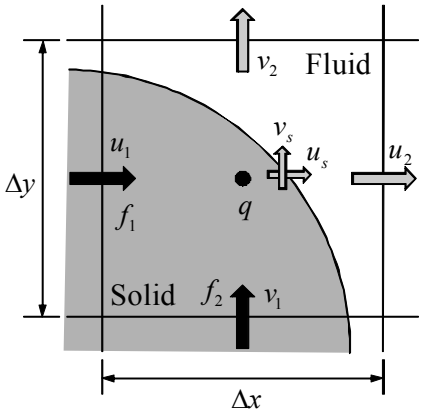

Fig. 1. Schematic diagram of immersed boundary method.

with non-zero f_i and zero elsewhere. In two dimensions (Fig. 1), the mass source/sink is given as

$$q = \frac{u_s^k - u_1^k}{\Delta x} + \frac{v_s^k - v_1^k}{\Delta y}. \tag{8}$$

More detailed procedures on how to obtain the momentum forcing and mass source/sink are shown in Kim *et al.* [3]

The u^k and v^k in Eq. (8) are unknown until Eq. (5) is solved, but they should be used to solve Eq. (4). Thus, $\hat{u}^k$ and $\hat{v}^k$ are used to determine q in Eq. (8), that is,

$$q = \frac{u_s^k - \hat{u}_1^k}{\Delta x} + \frac{v_s^k - \hat{v}_1^k}{\Delta y}. \tag{9}$$

For this reason, an error is generated from the continuity for the cell containing the immersed boundary:

$$e_2 = \frac{\hat{u}_1^k - u_1^k}{\Delta x} + \frac{\hat{v}_1^k - v_1^k}{\Delta y}. \tag{10}$$

In Eqs. (5) and (6), $u_i^k - \hat{u}_i^k = \vartheta(\Delta t^2)$ because $\phi = \vartheta(\Delta t)$, and thus $e_2 = \vartheta(\Delta t^2)$. This error does not cause any problem for flows with steady boundary conditions but may produce pressure oscillations and spurious velocities in the vicinity of the immersed boundary when an unsteady boundary condition is given on the immersed boundary. Therefore, this error should be eliminated or significantly reduced.

3. Remedy

As shown in Eq. (10), the error is proportional to the difference between the velocity and intermediate velocity on or near the immersed boundary (i.e., at the grid points where $f_i \neq 0$). This difference is $-2\alpha_k \Delta t\ \partial \phi^k / \partial x_i$ as in Eq. (5), and the error becomes zero when $\partial \phi^k / \partial x_i = 0$ there. Therefore, we apply this Neumann boundary condition on the grid points where the momentum forcing f_i is applied when we solve the Poisson Eq. (4). An example of applying this boundary condition is schematically drawn in Fig. 2 for flow over a circular cylinder.

4. Numerical examples

First, we consider a model problem shown in Fig. 3, where a jet is issued at the bottom center of the

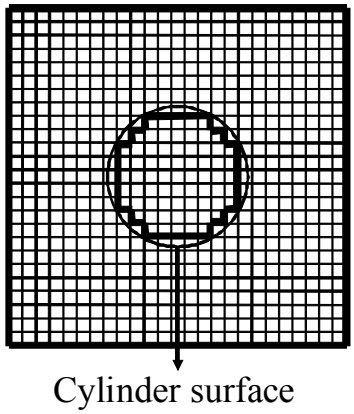

Fig. 2. Boundary condition for the Poisson Eq. (4). The thick solid lines denote the grid lines where the Neumann boundary condition is applied.

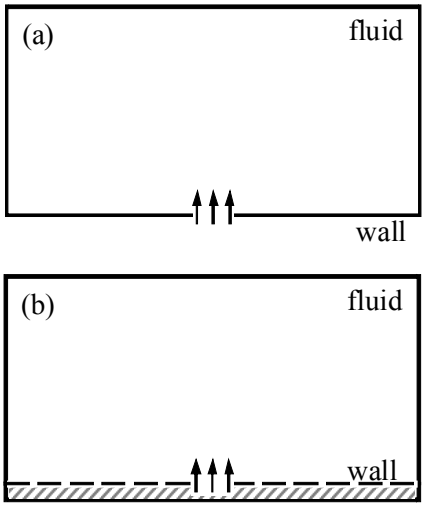

Fig. 3. Schematic diagram of model problem: (a) without IB method; (b) with IB method.

domain. The domain size of the fluid region is $20L \times 10L$, where L is the jet width. In Fig. 3(a) where the IB method is not applied, the following Dirichlet boundary conditions are applied on the bottom wall:

$$\begin{cases} v = 0 & \text{on } 0 \le x < 9.5L \text{ and } 10.5\text{L} < x \le 20L \\ v = v_{jet}(t) & \text{on } 9.5\text{L} \le x \le 10.5L \end{cases} \tag{11}$$

With the IB method (Fig. 3(b)), the bottom wall represented by the IB method is shown as the dashed line, and the area below the dashed line is the solid body.

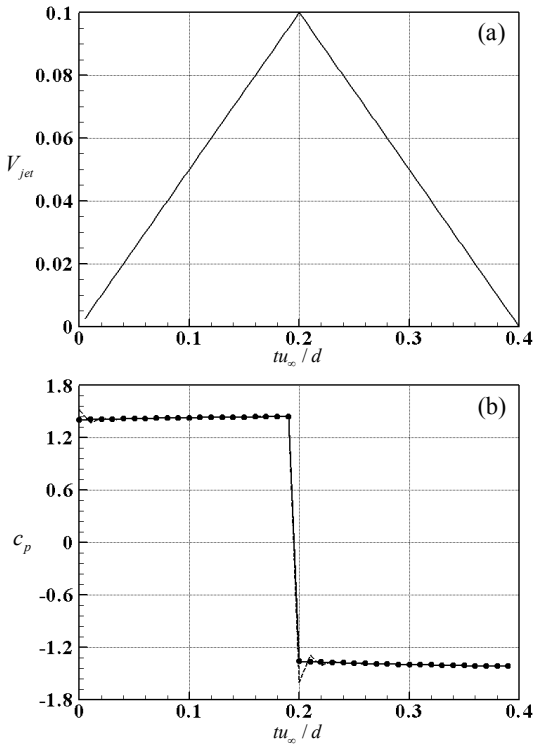

Fig. 4. Time histories of the jet exit velocity and pressure coefficient: (a) V_{jet} ; (b) c_p. In (b), —, without IB method; ···, with IB method and boundary treatment; - - -, with IB method but without boundary treatment.

For both cases, the fluid domains are identical to each other. The Reynolds number based on the jet exit velocity and width is 100. The initial velocity in the fluid domain is zero. The grids are non-uniformly distributed, and the numbers of the grid points are $150(x) \times 60(y)$ for Fig. 3(a) and $150(x) \times 64(y)$ for Fig. 3(b), respectively. An unsteady jet exit velocity is given in Fig. 4(a): the jet exit velocity linearly increases and then decreases in time. The pressure coefficients at the center of the jet exit with and without the present IB method are shown in Fig. 4(b) together with that with the IB method but without applying the Neumann boundary condition on the immersed boundary (in other words, no boundary condition is imposed on the immersed boundary for Eq. [4]). As shown, the pressure coefficient with the present boundary treatment works well, whereas artificial oscillations occur without the boundary treatment when the jet exit velocity suddenly changes in time.

The second example is the flow over a circular cylinder at a Reynolds number of 100 based on the

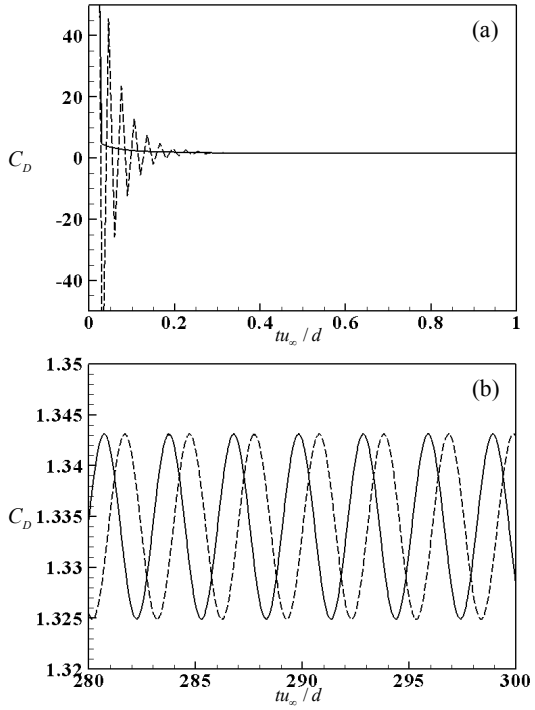

Fig. 5. Time histories of the drag coefficient: (a) $0 \le tu_\infty / d \le 1$; (b) $280 \le tu_\infty / d \le 300$. —, with the boundary treatment; - - -, without the boundary treatment.

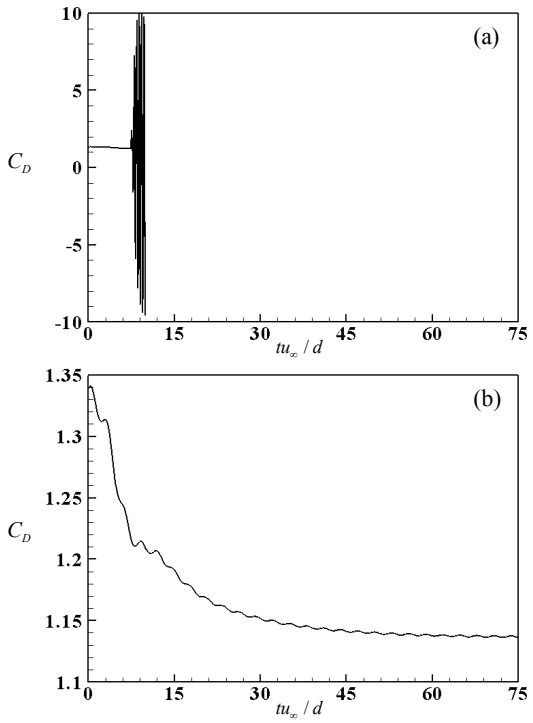

Fig. 6. Time histories of the drag coefficient: (a) without boundary treatment; (b) with boundary treatment.

free-stream velocity u_∞ and cylinder diameter d. The size of the computational domain is $70d \times 100d$. The number of grid points is 391×225 in the streamwise (x) and transverse (y) directions, respectively. A Dirichlet boundary condition ($u/u_\infty = 1$ and $v = 0$) is applied at the inflow and far-filed boundaries, and a convective boundary condition ($\partial u_i / \partial t + c \partial u_i / \partial x = 0$) is used for the outflow boundary, where c is the plane-averaged streamwise velocity at the exit.

Fig. 5 shows the time histories of the drag coefficient C_D obtained with and without the present boundary treatment. Here, the initial velocity condition at $t = 0$ is given as $u/u_\infty = 1$ and $v = 0$. Due to the no-slip condition on the cylinder surface imposed at $t = 0$, there are large artificial drag oscillations near $t = 0$ when the present boundary treatment is not used, whereas there is no such oscillation with the boundary treatment (Fig. 5(a)). After some time, there is no essential difference between the two solutions obtained with and without the boundary treatment (Fig. 5(b)) because there is no change in the boundary condition in time.

The last example is a feedback control of flow over a circular cylinder. The actuation is an unsteady blowing and suction from the cylinder surface and is determined from the distribution of the instantaneous surface pressure at each instant [4]. Thus, an artificial oscillation of surface pressure caused by the error e_2 in case of no boundary treatment results in a wrong actuation velocity, which again produces non-physical surface pressure and results in the blow-up of the numerical solution (Fig. 6(a)). On the other hand, with the present boundary treatment, the drag coefficient does not show such artificial behavior. The time averaged drag coefficient and the maximum lift fluctuation are 1.137 and 0.067, respectively, and they are in excellent agreement with those (1.142 and 0.066, respectively) from Min and Choi [4].

5. Summary

Through an IB method, artificial force oscillations on a solid body may occur when an unsteady boundary condition is given on the solid boundary. In the present study, we suggested a new boundary treatment on or near the immersed boundary when the

Poisson equation for the pseudo-pressure is solved. The Neumann boundary condition was applied for the pseudo-pressure at the grid points where the momentum forcing was applied. This boundary treatment effectively eliminated artificial force oscillations for the three flow examples.

Acknowledgment

This work was supported by the NRL (2009-0066334) Program of NRF, KRF Grant (KRF-2007-412-J03001) and WCU Program of the Ministry of Education, Science, and Technology, Korea. The CPU time was provided by "The Seventh Strategic Supercomputing Support Program".

References

[1] C. S. Peskin, The fluid dynamics of heart valves: Experimental, theoretical, and computational methods, *Annu. Rev. Fluid Mech.*, 14 (1982) 235.

[2] R. Mittal and G. Iaccarino, Immersed boundary method, *Annu. Rev. Fluid Mech.*, 37 (2005) 239.

[3] J. Kim, D. Kim and H, Choi, An immersed-boundary finite volume method for simulations of flow in complex geometries, *J. Comput. Phys.* 171 (2001) 132.

[4] C. Min and H. Choi, Suboptimal feedback control of vortex shedding at low Reynolds numbers, *J. Fluid Mech.* 401 (1999) 123.

Seung Jeon obtained his B.S. degree at the School of Mechanical and Aerospace Engineering, Seoul National University, Korea, in 2003. He is currently a Ph.D. candidate at the School of Mechanical and Aerospace Engineering, Seoul National University, Korea.

Haecheon Choi obtained his B.S. and M.S. degrees at the Department of Mechanical Engineering, Seoul National University, Korea, in 1985 and 1987, respectively. He received his Ph.D. degree from Stanford University in 1992. Dr. Choi is currently a professor at the School of Mechanical and Aerospace Engineering, Seoul National University. His research interests include turbulence, flow control, CFD, and bio-mimetic engineering.